RESEARCH ARTICLE

Analysis of Body-Fin Cooperative Propulsion Mechanism of Koi Carp Using Pose Estimation

Xin Wu[1,2], Yonghui Wang[3], Mingzhu Hua[4], Lianming Wang[1,‡]

ABSTRACT

With the rapid development of science and technology, advanced underwater robots have extensively promoted human beings' abilities to understand, explore, and preserve the oceans. Understanding the mechanism of fish movement has essential scientific and practical significance for advancing underwater robotics technology. On the one hand, it can reveal the secret of efficient swimming of fish and understand the behavior of fish; on the other hand, it can provide a basis for the research and development of new underwater robots with low noise, high efficiency, high stability, and high mobility. In this research, to analyze the synergistic propulsion mechanism of fish body and fins, a fish body-fin synergistic propulsion model is established to provide a theoretical basis for such analysis. A fish pose and motion estimation platform is constructed to provide data support. With the help of the constructed platform for quantifying the movement of a koi, fish wave characteristics are analyzed for three swimming states of the koi (advancing, retreating, and turning) and four swimming states of the koi (advancing, retreating, turning, and floating up) are summarized for the corresponding body-fin coordination mechanism. The proposed analysis method provides an innovative idea for fish movement research. The research results can significantly help the designing, developing, and optimizing modern underwater robots.

KEYWORDS: Fish, Body-fin Cooperative Propulsion mechanism, Pose estimation, Pose and Motion Estimation Platform

INTORDUCTION

With the rapid development of science and technology, the resource shortage problem is increasingly emerging, human beings have to turn their attention to the oceans. While the complex marine environment makes it difficult for humans to move freely underwater, underwater robots can work freely under such harsh conditions. Underwater robotics is an essential technique in marine oil and gas industry, defense sector, maritime search and rescue work, oceanographic research, underwater archaeology, and environmental monitoring Bogue (2015).

[1]School of Marine Information Engineering, Hainan Tropical Ocean University, Sanya, China
[2]Guangdong DyneChem Electronic Technology Co.,Ltd., Zhongshan, China
[3]Department of Computer Science, Prairie View A&M University, Prairie View, TX, USA
[4]School of Physics, Northeast Normal University, Changchun, China

‡Authors for correspondence: (lmwang@hntou.end.cn)

Received 1 May 2018; revised 5 December 2018

At present, underwater robots generally use electric propellers for propulsion. This type of robot usually adopts multiple propellers to ensure freedom of movement, but its shape and structure are complex, and its poor hydrodynamic and slewing performance.

After millions of years of evolution, fish have developed fast and efficient locomotion technology. Their mobility levels far exceed those of traditional engineered marine locomotion systems. Their excellent locomotion and coordination have made them a superb source of inspiration for engineers to design and control new underwater robots within the framework of bionics. The new type of underwater robot developed based on the swimming principle of fish and other aquatic lives will become a powerful tool to assist humans in exploring, monitoring, utilizing, and preserving the oceans Bandyopadhyay (2005); Yu et al. (2018).

"How do fish move?" This is an essential question for researching and developing new underwater robots. The answer to this question has important scientific significance and practical values. On the one hand, it helps humans to understand the biomechanical effects of fish swimming, then further understand fish behavior, physiology, and ecology. On the other hand, the mobility of fish provides the basis for the theory of research, which is of great significance to the design and control of new underwater robots.

In recent years, computer vision-based recognition, detection, and measurement technologies have continuously developed. With the help of such technology and a certain number of cameras, features of a target object can be extracted and utilized. Some studies on fish movement analysis using computer vision methods have already been proposed.

Wu Wu (2010) proposed a video tracking system for measuring the 3D kinematics of free-swimming fish. Wang et al. Wang et al. (2013) introduced a high-speed camera system to analyze two 3D movements of koi. Voesenek et al. Voesenek et al. (2016) proposed a method to track fish swimming in 3D using multiple high-speed camera video systems. Mao et al. Mao et al. (2016) discussed the basic technology of occlusion tracking, studied the matching model of actual and imaginary fish occlusion, and realized 3D fish target non-occlusion tracking. Siberian et al. Saberioon and Cisar (2016) developed multiple fish tracking systems based on currently available structured light sensors. Qian et al. Qian and Chen (2017) established a simple and economical device to detect the 3D motion of zebrafish, enabling scientists to track the 3D motion of multiple zebrafish at a low cost and with precise spatial location. Cheng et al. Cheng et al. (2018) proposed a method for quantitatively measuring 3D motion trajectories of fish based on a three-camera imaging system, tracking fish in the main view with the help of convolutional neural networks, and formulating cross-view data association with temporal linearity. Liu et al. Liu et al. (2019) proposed a skeleton-based 3D tracking method for fish schools.

These traditional fish motion video analysis methods mainly focus on 2D/3D motion tracking and simple motion pattern analysis of fish. These analytical methods lack the analysis of fish movement posture, such as how the caudal or pectoral fins work together during movement. The main reason for the lack of relevant research is that it is challenging to extract such motion features due to the disordered motion of animals or animal limbs. The features extracted by traditional image processing methods are insufficient to analyze local complex motions. A more efficient tool to extract more information (features or patterns) for analyzing local complex motions is desired. Such a method can extract more features and be applied to more scenes to solve earlier problems.

In recent years, the rapid development of deep learning-based computer vision technology has made it efficient for solving complex feature extraction problems. Deep learning models can quickly obtain the position and attitude of the target object in the target coordinate system. In computer vision, pose estimation is defined as identifying specific objects in an image and determining the position and orientation of each object relative to a particular coordinate system. To sum up, fish movement is complex and unpredictable. Establishing a hydrodynamic model that can fully describe fish movement is difficult. In addition, extracting movement features based on traditional computer vision techniques is complex, and the extracted features are not enough to analyze local areas. Complex motion problems need to be solved urgently in fish motion analysis research.

Considering that pose estimation can detect the two-dimensional image coordinates (2D pose estimation) or the three-dimensional world coordinates (3D pose estimation) of a target object, applying it to the quantification of fish motion may be able to solve the problems existing in the current research. Therefore, this study intends to solve the fish motion analysis problem with the help of pose estimation based on modern computer vision technology. The quantitative analysis provides data support for analyzing the synergistic propulsion mechanism of fish body and fins. This paper proposes a model that can describe the synergistic propulsion of fish body and fins as comprehensively as possible to provide a theoretical basis for fish motion analysis. To sum up, our main contributions to this research include three aspects:

(1) A fish pose and motion estimation platform is built for fish motion research. The platform mainly includes fish movement data collection, processing, and visualization.
(2) Fish body waves are studied, and a discrete model of fish body-fin synergistic propulsion is established as a theoretical basis for studying fish movement.
(3) Taking a koi as the experimental research object, the platform is used to obtain the fish movement characteristics. The fish movement is analyzed combined with the established model. Finally, the koi's body-fin coordination mechanism of four swimming states (advancing, retreating, turning, and floating) is analyzed and summarized.

The fish movement research platform constructed in this study provides a new method for fish movement research, and the research results of koi movement have specific reference significance for underwater robotics research.

MATERIALS AND METHODS

Fish and experimental setups

The experiments were performed using a koi carp, which is a subcarangiform swimmer. The carp (body length $L = 300$ mm) was housed in a water tank in the laboratory. The fish pose and motion estimation platform, which is illustrated in Fig. 1, was constructed with high frame rate cameras plus the support of pose estimation based motion parameter measurement algorithm Wu et al. (2022). The platform consists of the following equipment: a water tank (120 cm × 20 cm × 30 cm in length, width, and depth, respectively), a high-performance computer, 3 high-frame-rate (210 FPS) and high-resolution (1280 × 1024 pixels) CCD cameras, a wave maker, and 2 fill lights (maximum power 100 W). Example images captured by the 3 cameras are shown in Fig. 2. All videos recorded by the three cameras were sent to the computer and stored in the computer's hard drive.

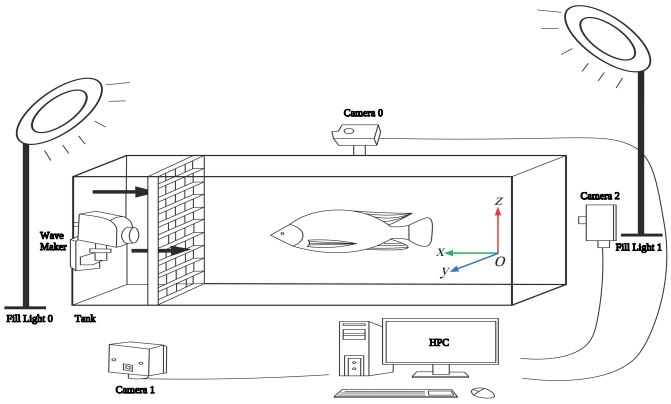

Fig. 1. Schematic diagram of fish pose and motion estimation platform.

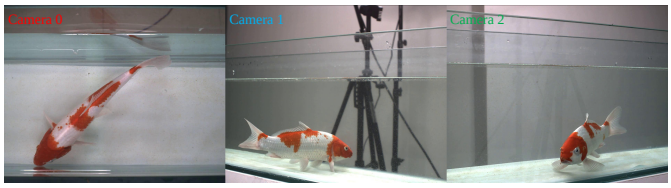

Fig. 2. Examples of captured images.

Once the koi's original motion data is obtained, the koi's motion and pose parameters (displacement, velocity, pose angle, and vibration frequency) are extracted using the motion parameter measurement method Wu et al. (2022) based on pose estimation. These parameters can then be used to analyze the motion of the koi.

The graphical interface for pose estimation and motion parameter visualization, as shown in Fig. 3, is designed to facilitate data processing and motion visualization. The graphical interface is divided into primary and plug-in windows. The main window mainly visualizes changing motion parameters with time, and the plug-in window mainly visualizes the selected key points' postures and motion parameters. The interface runs stably and can independently select multiple key points for visualization.

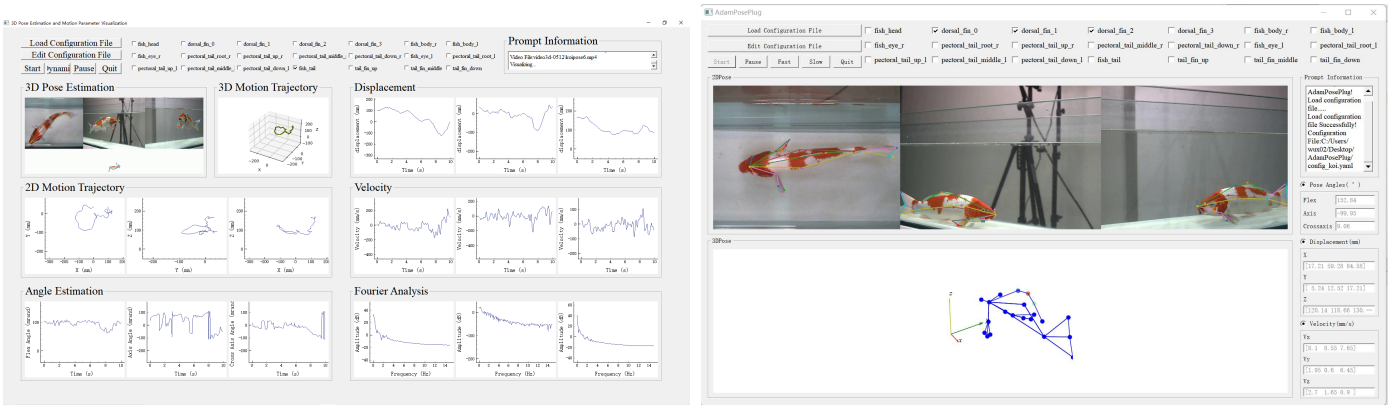

(a) (b)

Fig. 3. The graphical interface for fish movement data processing and visualization: (a) the main window and (b) the plug-in window.

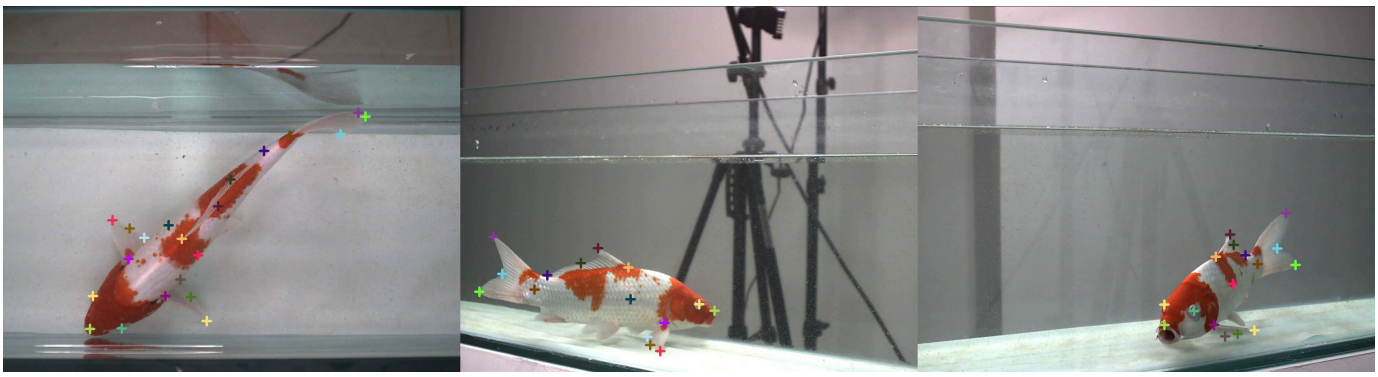

Fig. 4. An example diagram of key points labeling of the koi.

To analyze the koi motion, as shown in Fig. 4, twenty-one key motion points are selected for labeling on the carp based on our estimation results: one on its head, one on each eye, four on its back, four on each pectoral fin, one on each side of the body, and four on the caudal fin. For more dynamic display results and detailed software information, please refer to the software engineering of this research to https://github.com/wux024/AdamPose and https://github.com/wux024/AdamPosePlug.

The fish pose and motion estimation platform integrates data collection, processing, and analysis. The input is a video of fish moving in the tank from multiple perspectives, while the outputs are 2D and 3D pose estimations and motion parameters (2D/3D motion trajectory, displacement, velocity, acceleration, pose angle, and Fourier transformation). This platform provides solid data support for fish motion analysis. In this study, only movements of the koi in still water is studied, no flow and waves were created.

Fish wave model

Fish perform swimming by bending and swinging their bodies and fins . A diagram of fish body wave curve is shown in Fig. 5. According to the observation results of fish in the BCF (Body and/or Caudal Fin) modelWestneat et al. (1993), the expression of fish body wave $y(x,t)$ obtained by fitting is:

$$y(x,t) = (c_0 + c_1 x + c_2 x^2)\sin(2\pi f t + kx) \tag{1}$$

where $y'(x) = c_0 + c_1 x + c_2 x^2$ is the envelope equation of the fish body wave, x represents the coordinates of any point on the fish body, c_0, c_1, and c_2 are envelope coefficients. The network coefficient, k, is the fish wave number and f is the caudal fin swing frequency.

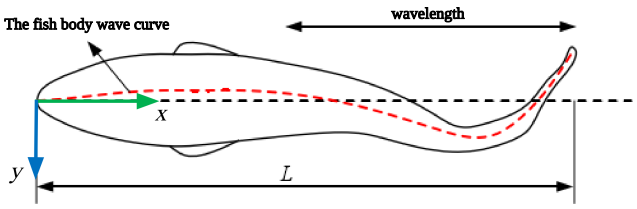

Fig. 5. Schematic diagram of fish body wave curve.

In addition, for more than 75% of fish involved in swing, the fish body wave is in the form of a traveling wave with a gradually increasing amplitude, and there is another expression:

$$y(x,t) = A_0 e^{a(\frac{x}{L}-1)} \sin\left[\frac{2\pi}{\lambda}(vt + x)\right] \tag{2}$$

where A_0 is the fish body wave swing coefficient, a is the amplitude growth coefficient, λ is the fish body wave wavelength, and v is the fish body wave speed.

If the fish body is modeled more accurately, more complete fish wave characteristics can be obtained. For example, the fish body wave model established based on viscoelastic beam theory can analyze the swimming situation of fish from the inside of the fish body Valdivia y Alvarado (2007); Nguyen et al. (2013), and its dynamic equation is a high-order partial differential equation Weaver Jr et al. (1991). This type of model describes the complex modal characteristics of the fish wave. Its establishment involves relatively complex biomechanical principles, which is beyond the scope of this study. The main focus of this study is the experimental research method for analyzing biological motion. Without going into details, it is worth noting that an in-depth study of biomechanical principles can help design more accurate experiments.

A discrete model for fish body-fin synergistic propulsion

In the underwater environment where fish live, the water currents are not stable, especially in the oceans. Due to the existence of waves, internal waves, currents, eddies, and other fluid phenomena, the water currents are not identical at different spatial locations, and they constantly change over time. In this complex water environment, fish rely on synergistic oscillations or fluctuations between their bodies and fins (pectoral, dorsal, caudal, ventral, and anal fins) to achieve free swimming, such as advancing, retreating, turning, floating up, sinking, and hovering. In this section, a discrete model is developed to describe the synergistic propulsion of fish body and fins qualitatively.

Firstly, the water flow environment where the fish is located can be defined as $\mathcal{E}$, and $\mathcal{M}$ ($m_i \in \mathcal{M}$) can be used to represent the fish swimming category set, where m_i may be advancing, retreating, turning, floating up, sinking, hovering, etc. Secondly, all observed parts form a target set which is defined as $\mathcal{F}$ ($f_j \in \mathcal{F}$), here f_j can be the caudal fin, left pectoral fin, right pectoral fin, left pelvic fin, right pelvic fin, anal fin, dorsal fin, etc. The fish body is defined as set $\mathcal{B}$. Finally, all possible states of the fish body parts, such as the fish body and each fin, are defined as a state set $\mathcal{P}$ ($p_k \in \mathcal{P}$), where p_k can be swing left, swing right, rapid swing, flapping up and down, paddling back and forth, clockwise rotation, counterclockwise rotation, left tilt, right tilt, static, fin surface fluctuates downstream, fin surface fluctuates upstream, etc. The set elements can increase or decrease based on the actual observation results.

Therefore, a fish swimming event can be expressed as, in time period T, under the water flow environment $\mathcal{E}$, the fish body $\mathcal{B}$ and each fin $\mathcal{F}$ being in certain state $\mathcal{P}$ work together to produce fish swimming $\mathcal{M}$. A state matrix $\mathcal{S}_t$ can be used to represent the state $\mathcal{P}_\mathcal{B}$ of the fish body $\mathcal{B}$ and the state of each fin, at a moment t. The rows of the matrix are determined by the target set $\mathcal{F}$, and the columns of the matrix are determined by the pose set $\mathcal{P}$, so the dimension of the matrix should be $|\mathcal{F}| \times |\mathcal{P}|$. An element s_{jk} of the matrix indicates whether fin f_j is in state p_k or not depending on whether $s_{jk} = 1$ or $s_{jk} = 0$. Therefore, the swimming state of the fish in time period T can be represented by

$$\mathcal{M} = \sum_{\mathcal{S}_t} \mathcal{E}(\mathcal{P}_\mathcal{B}, \mathcal{S}_t). \tag{3}$$

This formula shows that the swimming of a fish is a cumulative effect of various states produced by water current forced movements of the fish body and each fin over a time period. For example, a fish swimming forward in a straight line is resulted from a relatively regular swing of the body or pectoral fins for a certain time period.

Thus, by measuring the states of a fish in time period t with relevant technologies, fish swimming can be characterized to a certain extent. For example: in a certain time period of t, when the water flow environment is ε, the swimming state is m_i, and the fish body posture is $p^i_\mathcal{B}$, the state of each fin can be represented using state matrix $\mathcal{S}_t$, as shown in Table 1.

Assuming there is a measurement system which can obtain $\mathcal{S}_t$ for any time period t, then after N measurements, the number of $s_{jk} = 1$ to N ratio represents, when the fish body posture is $p^i_\mathcal{B}$, the frequency of fin f_j being in state p_k. A larger ratio value will cause effect m_i. Therefore, the qualitative description of the body-fin propulsion of fish swimming can be determined by using statistical laws. Combining with continuous mathematical model, the mechanism of fish body-fin synergistic propulsion can be described more completely.

RESULTS AND DISCUSSIONS

The length of the koi in this research is about 30 cm. Combining with theoretical models and experimental data, the mechanism of synergistic propulsion of fish body and fins is analyzed from different perspectives. In this study, the experimental platform was used to simultaneously record 40-minute motion videos of the koi from three different angles. The videos were divided into 10-second segments for a total of 240 videos. The experiment is mainly divided into two parts:

(1) Using the fish body wave model to analyze the fish body wave characteristics in different 3 swimming states (advancing, retreating, and turning); and
(2) using the discrete model to analyze body-fin coordination of the koi in 4 different swimming states (advancing, retreating, turning, and floating up) and to determine the state tables of the koi in different swimming states and the motion parameters to maintain these states.

Fish wave analysis of the koi

This section mainly observes the fish body waves of the three swimming states of the koi: advancing, retreating, and turning. The fish body waves of these three motion states are the easiest ones to observe and relatively close to the ideal fish body waves.

Koi fish body wave analysis for advancing The advancing state of the koi over a time period is shown in Fig. 6a. The first row in the figure shows consecutive frames of the actual viewing angle, and the second row shows the 3D pose estimations from a virtual perspective. Both rows show slight bending of the fish body. Pose estimation quantifies motion parameters for analyzing fish body waves as koi advances.

A total of 5 points, marked on the back of the fish at the locations of $x = 0.11, 0.15, 0.17, 0.21, 0.30$ m, are selected for the analysis. The y direction displacements of these points are shown in Fig. 6b, which are plotted along the time axis.

According to equation (1), ideally, at any point of the fish body, the displacement in y direction should be a sine wave, which is quite different from the actual measurement. The main reason is that the fish does not move periodically according to the ideal advancing direction. By comparing the curve with the actual swimming video, it is found that the fish body movement is in line with the actual situation.

Table 1. State matrix $\mathcal{S}_t$

$\mathcal{E}$	$\mathcal{M}$	$\mathcal{P}_{\mathcal{B}}$	$\mathcal{F}$ \ $\mathcal{P}$	p_1	p_2	$\cdots$	p_k	$\cdots$
			f_1	s_{11}	s_{12}	$\cdots$	s_{1k}	$\cdots$
			f_2	s_{21}	s_{22}	$\cdots$	s_{2k}	$\cdots$
ε	m_i	$p^i_{\mathcal{B}}$	$\vdots$	$\vdots$	$\vdots$	$\ddots$	$\vdots$	$\vdots$
			f_j	s_{j1}	s_{j2}	$\cdots$	s_{jk}	$\cdots$
			$\vdots$	$\vdots$	$\vdots$	$\vdots$	$\vdots$	$\cdots$

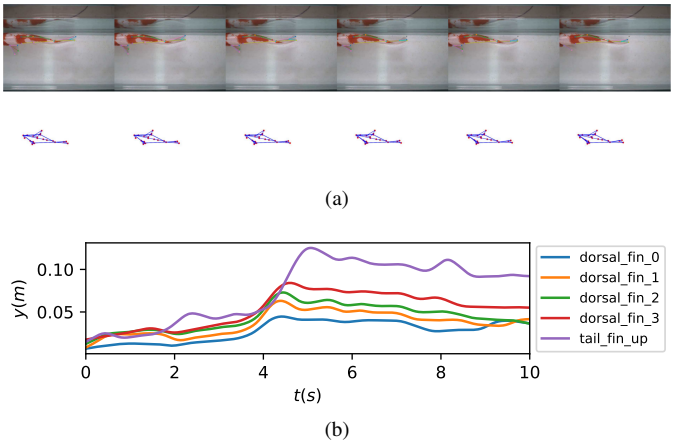

Fig. 6. Fish body wave analysis for the koi advancing state: (a) consecutive frames showing fish poses and the 3D pose estimation from the virtual perspective; and (b) the actual fish body wave curve of the koi advancing state.

Koi fish body wave analysis for retreating The actual motion of the koi's retreating state during a time period and the 3D pose estimation of the virtual perspective are shown in Fig. 7a. The same key points of observation are used. The displacement curves of these points in y direction along time axis are shown in Fig. 7b. For retreating, the swing of the fish body is not big, instead the body has a small amplitude quasi-periodic swing. The main driving parts for retreating are the left and right pectoral fins. Subsequent experiments will carry out a detailed analysis of this state.

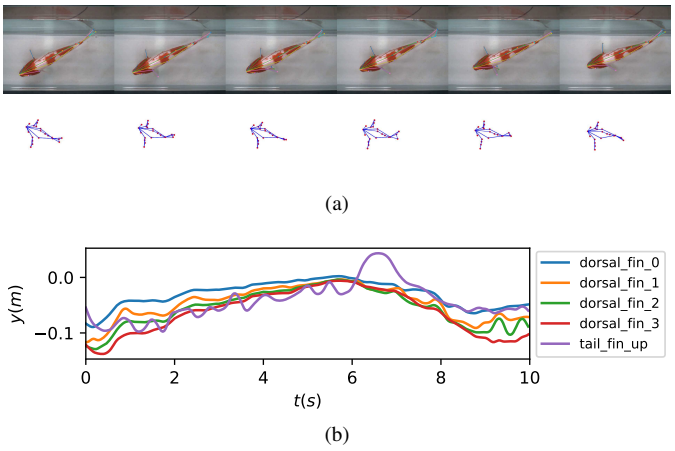

Fig. 7. Fish body wave analysis for the koi retreating state: (a) consecutive frames showing fish poses and the 3D pose estimation from the virtual perspective; and (b) the actual fish body wave curve of the koi retreating state.

Koi fish body wave analysis for turning The top view of the actual motion status of the koi turning state in a period of time and its 3D pose estimation are shown in Fig. 8a. The key points observed are the same as those in the previous two states. The displacements of the points in y direction along time axis are shown in Fig. 8b. For turning, the fish body first has a slow adjustment process, then swings wildly, and finally, after the turning is completed, the fish body swings and adjusts slightly. The primary body parts for turning are the fish body and the caudal fin, while the other fins have little effects and do not provide significant driving forces. Subsequent experiments will give more detailed body-fin coordination.

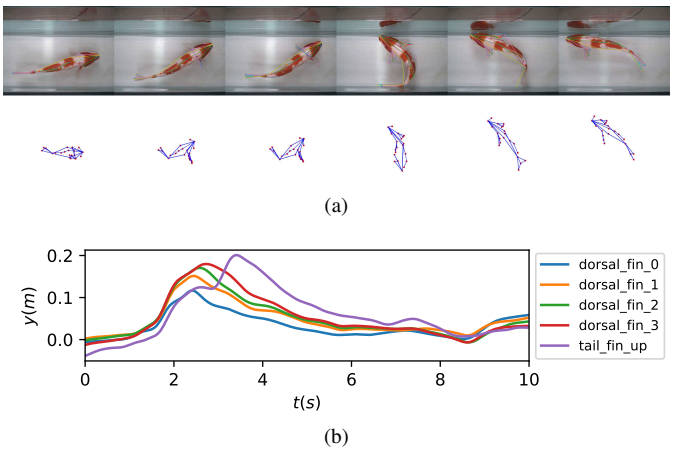

Fig. 8. Fish body wave analysis for the koi turning state: (a) consecutive frames showing fish poses and the 3D pose estimation from the virtual perspective; and (b) the actual fish body wave curve of the koi turning state.

Body-fin synergistic propulsion mechanism analysis

This section mainly measures the state transition matrix of four koi swimming states: advancing, retreating, turning, and floating up, and gives the motion parameters for each fin. The body-fin coordination process of sinking is similar to that of floating up, so no measurement for sinking is conducted. In addition, hovering is mainly adjusted by the fish body's internal buoyancy or small fluctuations, which is not within the scope of research on the body-fin synergistic propulsion mechanism.

In this study, the experimental conditions are: water flow environment $\mathcal{E}$ = **still water**; and swimming category set $\mathcal{M} = \{m_1$ (advancing), m_2 (retreating), m_3 (turning), m_4 (floating up), m_5 (sinking), m_6 (hovering)$\}$. The main fish body parts being observed are fish body $\mathcal{B}$ and fins $\mathcal{F} = \{f_1$ (caudal fin), f_2 (left pectoral fin), f_3 (right pectoral fin)$\}$. The movement state set for

Journal of Experimental Biology (2019) 00, jebxxxxxx. doi:10.1242/jeb.xxxxxx

Table 2. Koi advancing status table

$\mathcal{E}$	$\mathcal{M}$	$\mathcal{P}_{\mathcal{B}}$	$\mathcal{F}$ \ $\mathcal{P}$	p_1	p_2	p_3	p_4	p_5
still water	m_1	$p_2 + p_4/p_5$	f_1	0	1	0	1/0	1/0
			f_2	1/0	0	1/0	0	1/0
			f_3	1/0	0	1/0	0	1/0

fins is defined as $\mathcal{P} = \{p_1$ (slap back and forth), p_2 (slap left and right), p_3 (slap up and down), p_4 (big flap), p_5 (small flap)$\}$.

Synergistic analysis of body and fins for koi advancing By analyzing the state of the fish advancing frame by frame in 240 videos, the state table tabulated in Table 2 exhibits the highest frequency, thus Table 2 shows the state table S_t for koi advancing, where $1/0$ indicates whether the state is present or not. Table 2 qualitatively describes the cooperation between the fish body and the three fins, which play a significant role when the koi moves forward. When the koi swims forward, the fish body will swing left and right in a large or small movement ($p_2 + p_4/p_5$), and at the same time the tail fin swings with the fish body in a large or small flap, which is the main driving force for the koi to move forward. In most cases, the left and right pectoral fins adjust the forward posture through small back and forth strokes or up and down flaps, mainly to maintain the straight forward path and the position in the vertical direction. The following is a quantitative analysis of the body-fin coordination of the koi when it moves forward.

The plots of the movement parameters of the key points of the fish body and the key points of each fin (labeled as in Fig. 4) when the koi moves forward can be used to quantitatively analyze the body-fin coordination. Fig. 9 shows the displacement curves of the four key points of the fish body relative to the fish head, the displacement curves of the three outer key points on the caudal fin relative to the base of the caudal fin, and the displacement curves of the outer key points on the left and right pectoral fins relative to the corresponding bases of the left and right pectoral fins. Each row shows the $s - t$ curves of different key points relative the same body part in the three directions of x, y and z. Fourier analysis of these curves approximates the flap frequency.

From Fig. 9, it can be seen that, when the koi swims forward, the fish body slowly makes big swings in y direction, and the maximum swing amplitude exceeds 7.5 cm. At the same time, the caudal fin either sways extensively in y direction together with the fish body or sways slightly not synchronized with the fish body. The maximum sway of the caudal fin exceeds 3 cm, and the frequency of its big swings is about 0.25 Hz, while the frequency of the small swings is about 1.67 Hz. The left and right pectoral fins flap slightly back and forth and up and down. The maximum amplitude of the back and forth flaps exceeds 2 cm, and the flap frequency is about 0.167 Hz. The maximum amplitude of the up and down flaps exceeds 2 cm, and the flap frequency is about 0.89 Hz.

In addition, when fish swims, each fin will deform, and the pose angle can be used to measure the bending degree of each fin. The visual result of the deformation measurement of each fin is shown in Fig. 10. From Fig. 10, it can be seen that the koi fins deform when the fish swims forward. According to the definition of attitude angle, the first column of the figure represents the flexion and extension angle, and the variation range of the caudal fin flexion and extension angle is $95.0^\circ \sim 116.8^\circ$. The variation range of the left pectoral fin flexion and extension angle is $123.0^\circ \sim 140.4^\circ$, and the range of the right pectoral fin flexion and extension angle is

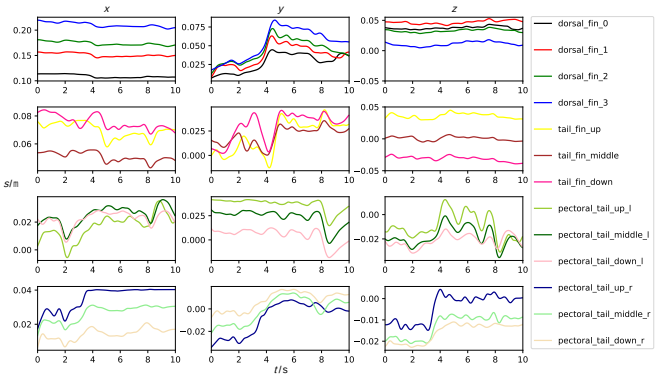

Fig. 9. Relative displacement measurements of 13 key points as the koi moves forward. The first row represents the change of the fish body; the second row represents the change of the caudal fin; the third row represents the change of the left pectoral fin; and the fourth row represents the change of the right pectoral fin.

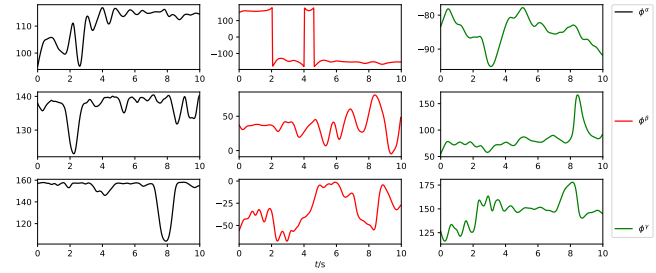

Fig. 10. The deformation measurements of each fin when the koi moves forward. The first row is the deformation of the caudal fin; and the second and third rows are the deformation of the left and right pectoral fins, respectively.

$103.9^\circ \sim 158.1^\circ$. The second and third columns of the figure represent complex rotations, which are directional and more complex deformations. These complex deformations are mainly to maintain the balance of the fish and control the direction of its movement.

Synergistic analysis of body and fins for koi retreating The fish body parts to be measured are the same as those for fish advancing. By analyzing the state of fish retreating frame by frame in the 240 videos, the state table tabulated in Table 3 exhibits the highest frequency, thus Table 3 is the koi retreating state table S_t, where $1/0$ in the table indicates whether the state is present or not. Table 3 qualitatively describes the coordination of the fish body, caudal fin, and pectoral fins when the koi moves backward. When the koi retreats, because the koi cannot look back, its body's displacement in y direction is relatively large without swinging left and right. The caudal fin hardly wiggles, and the pectoral fins are the primary drive for the koi's retreat. In most cases, the left and right pectoral fins adjust the retreat posture and provide the main drive through small back and forth strokes or up and down flaps. The fish moving speed is slow when it retreats, because the power provided by the pectoral fins is not sufficient. A quantitative

Table 3. Koi retreat status table

$\mathcal{E}$	$\mathcal{M}$	$\mathcal{P}_{\mathcal{B}}$	$\mathcal{F}$ \ $\mathcal{P}$	p_1	p_2	p_3	p_4	p_5
still water	m_2	hardly move	f_1	0	0	0	0	0
			f_2	1/0	0	1/0	0	1/0
			f_3	1/0	0	1/0	0	1/0

analysis of the body-fin coordination of the koi when it retreats is provided below.

It can be seen from Fig. 11 that, when the koi swims backward, the caudal fin does not have apparent periodic movement, but it has high deformation frequency. The left pectoral fin flaps back and forth with relatively high frequency, the maximum swing amplitude is about 2 cm, and the swing frequency is about 2 Hz. In addition, its up and down stroke amplitude exceeds 2 cm and the stroke frequency is about 2.5 Hz. The right pectoral fin is not highly synchronized with the left pectoral fin. Its back and forth stroke frequency is high, the maximum swing amplitude is about 3 cm and the swing frequency is about 1.32 Hz, while the up and down flap amplitude is about 2 cm and the flap frequency is about 1.5 Hz. The asynchrony of the left and right pectoral fins is one of the main reasons for its tortuous moving path as the fish retreats.

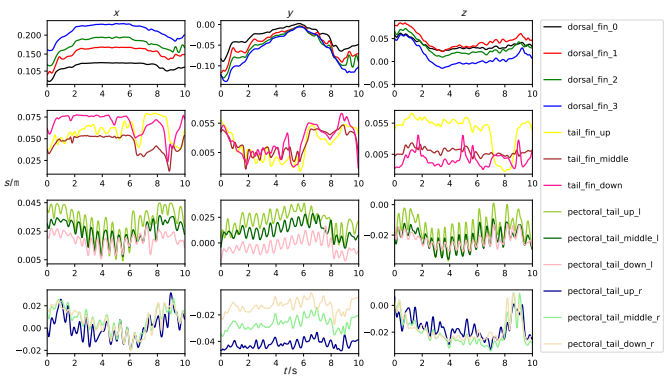

Fig. 11. Relative displacement measurements of 13 key points as the koi moves backward. The first row represents the change of the fish body; the second row represents the change of the caudal fin; the third row represents the change of the left pectoral fin; and the fourth row represents the change of the right pectoral fin.

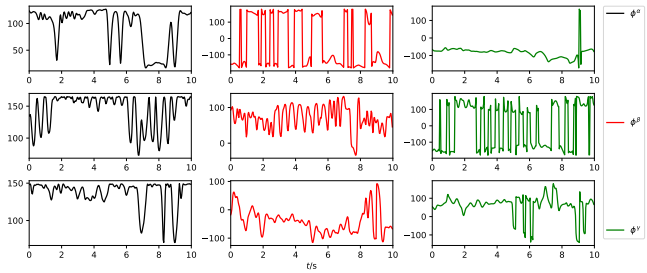

Fig. 12. The deformation measurements of each fin when the koi moves backward. The first row is the deformation of the caudal fin; and the second and third rows are the deformation of the left and right pectoral fins, respectively.

It can be seen from Fig. 12 that, in the process of retreating, the koi fins deform with relatively high deformation frequency. The range of flexion and extension angle of the caudal fin is $16.8^\circ \sim 126.9^\circ$; the range of flexion and extension angle of the left pectoral fin is $73.2^\circ \sim 165.3^\circ$; and the range of flexion and extension angle of the right pectoral fin is $70.5^\circ \sim 149.3^\circ$. The second and third columns of the figure represent complex rotations, which are directional and more complex deformations. These complex deformations are mainly to maintain the balance of the fish and control the direction of its retreat.

Synergistic analysis of body and fins for koi turning The same fish body parts as those used for analysis of fish advancing are used. Through the frame-by-frame analysis of the fish body turning videos, the status table as tabulated in Table 4 has the highest frequency, thus the state table S_t for koi turning is shown in Table 4, here $1/0$ in the table indicates whether the state is present or not. Table 4 qualitatively describes the coordination between the fish body, caudal fin, and pectoral fins when the koi turns. When the koi turns, the fish body bends considerably and the tail fin also bends significantly together with the fish body with a relatively high frequency. The pectoral fins do not play significant roles in the turning process, and their small up and down flaps are mainly to maintain the fish posture. The following is a quantitative analysis of the body-fin coordination for koi turning.

When the koi turns to the left, the fish body bends considerably $(p_1 + p_4)$. As can be seen from Fig. 13, together with the fish body, the tail fin bends considerably with a high frequency. The entire turning process is completed in about 4 s, and the swing range of the tail fin is about 12 cm. During this left turning process, the right pectoral fin is retracted to its belly, and the left pectoral fin is kept away from the belly to maintain the balance of the fish body through deformations. For turning, it mainly depends on its body's sudden movement, while the fins mainly balance and control the turning direction.

Fig. 14 reflects the deformations of the koi fins in the turning process. The variation range of caudal fin flexion and extension angle is $102.2^\circ \sim 127.1^\circ$, the variation range of left pectoral fin flexion and extension angle is $94.6^\circ \sim 164.6^\circ$, and the variation range of right pectoral fin flexion and extension angle is $53.7^\circ \sim 152.0^\circ$. The second and third columns of the figure represent complex rotations, which are directional and more complex deformations. These complex deformations are mainly to maintain the fish's balance and control its turning direction.

Synergistic analysis of body and fins for koi floating up Fig. 15 shows consecutive frames from a video of the koi floating up. As shown in the figure, the first three rows are consecutive frames of the actual observation perspectives, and the last row is the 3D pose estimation under the virtual perspective.

By analyzing the state of the fish floating up frame by frame in the 240 videos, the frequency of the state table tabulated in Table 5 is the highest. Therefore, the koi floating up state table S_t is shown in Table 5, where $1/0$ in the table indicates whether the state is present or not. Table 5 qualitatively describes the coordination of the fish body, tail fin, and pectoral fins when the koi floats up. When the koi floats up, the fish body swings slightly from side to side $(p_1 + p_5)$, while the tail fin follows the fish body and swings

Journal of Experimental Biology (2019) 00, jebxxxxxx. doi:10.1242/jeb.xxxxxx

Table 4. Koi turning status table

$\mathcal{E}$	$\mathcal{M}$	$\mathcal{P}_{\mathcal{B}}$	$\mathcal{F}$ \ $\mathcal{P}$	p_1	p_2	p_3	p_4	p_5
still water	m_3	$p_1 + p_4$	f_1	1	0	0	1	0
			f_2	0	0	1/0	0	1/0
			f_3	0	0	1/0	0	1/0

Table 5. Koi floating up status table

$\mathcal{E}$	$\mathcal{M}$	$\mathcal{P}_{\mathcal{B}}$	$\mathcal{F}$ \ $\mathcal{P}$	p_1	p_2	p_3	p_4	p_5
still water	m_4	$p_1 + p_5$	f_1	0	1	0	0	1
			f_2	1/0	0	1/0	0	1
			f_3	1/0	0	1/0	0	1

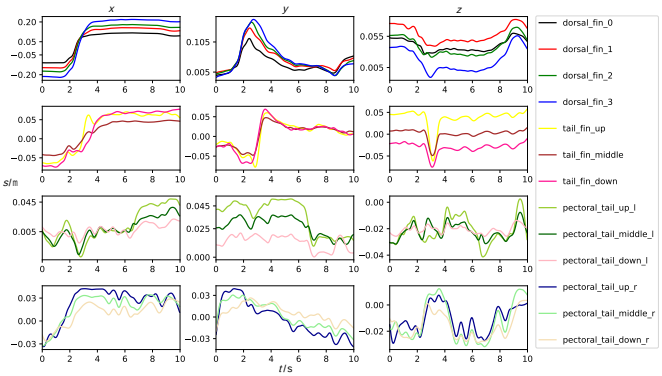

Fig. 13. Relative displacement measurements of 13 key points as the koi turns. The first row represents the change of the fish body; the second row represents the change of the caudal fin; the third row represents the change of the left pectoral fin; and the fourth row represents the change of the right pectoral fin.

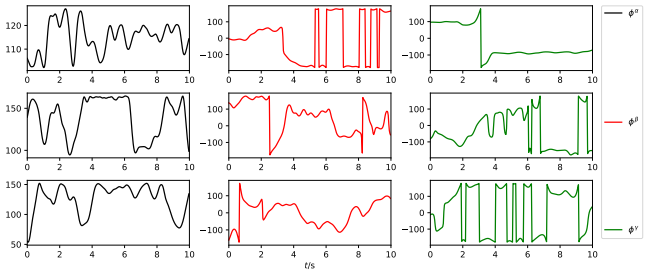

Fig. 14. The deformation measurements of each fin when the koi turns. The first row is the deformation of the caudal fin; and the second and third rows are the deformation of the left and right pectoral fins, respectively.

with small amplitudes but relatively high frequency. With small flapping, the pectoral fins play important role in the floating up process, they help the fish to maintain the posture and provide certain driving force. The following gives a quantitative analysis of the body-fin coordination for koi floating up.

It can be seen from Fig. 16 that, when the koi floats up, the fish body swings left and right at big amplitude, the maximum swing amplitude is about 8 cm, and the swing frequency is about 0.4 Hz. The caudal fin moves with the fish body at small amplitude, the maximum amplitude of the movement is about 5 cm, and the movement frequency is about 0.4 Hz. The swing amplitudes of the pectoral fins are negligible. Their maximum swing amplitude is about 2 cm, the swing frequency of the left pectoral fin is

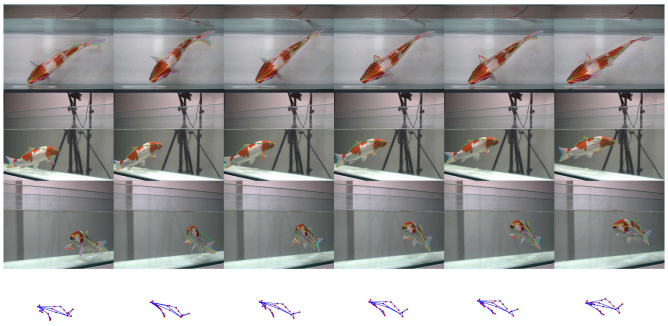

Fig. 15. An example of 3D pose estimation from different views and a virtual perspective when the koi floats up.

about 1.5 Hz, while the swing frequency of the right pectoral fin is 1.2 Hz.

Fig. 17 reflects the koi fins deformations in the floating up process. As shown in the first column, the variation range of caudal fin flexion and extension angle is $87.9^\circ \sim 133.1^\circ$, the variation range of left pectoral fin flexion and extension angle is $51.6^\circ \sim 167.0^\circ$, and the variation range of right pectoral fin flexion and extension angle is $58.1^\circ \sim 157.4^\circ$. The flexion and extension angle variations of the fins for floating up are far more severe than those for the previous three motion states. The second and third columns of the figure represent complex rotations, which are directional and more complex deformations. These complex deformations are mainly to maintain the balance of the fish and control its direction of floating up.

In this section, using the quantitative results of the fish attitude and motion estimation platform, combining with the established fish body-fin synergistic propulsion discrete model, the body-fin synergistic propulsion mechanism of the four koi swimming states in still water is analyzed. The body-fin synergistic propulsion mechanism provides qualitative and quantitative descriptions for koi swimming and demonstrates the validity of the proposed motion estimation based method for analyzing fish body-fin synergistic propulsion mechanism. For a L length koi swimming in still water, the body-fin coordination mechanism in four swimming states (advancing, retreating, turning, and floating up) is summarized as follows.

(1) When the koi moves forward, the fish body swings left and right with amplitude $A_1 < 0.34L$, and the swing frequency is

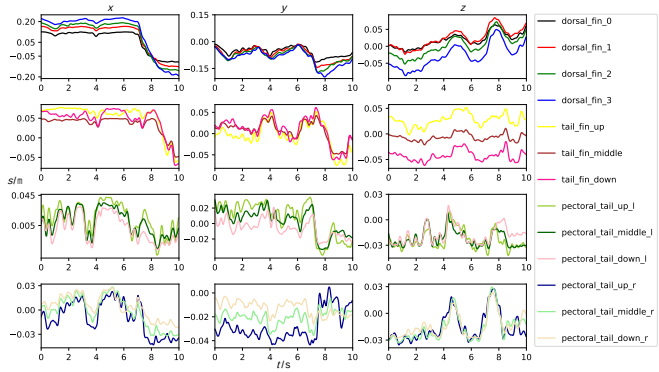

Fig. 16. Relative displacement measurements of 13 key points as the koi floats up. The first row represents the change of the fish body; the second row represents the change of the caudal fin; the third row represents the change of the left pectoral fin; and the fourth row represents the change of the right pectoral fin.

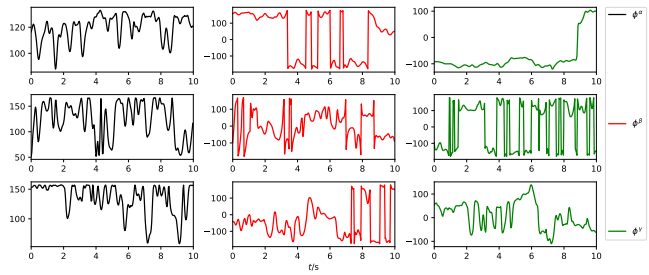

Fig. 17. The deformation measurements of each fin when the koi floats up. The first row is the deformation of the caudal fin; and the second and third rows are the deformation of the left and right pectoral fins, respectively.

0.28 Hz< f_1 <0.67 Hz. At the same time, the tail fin swings together with the fish body at an amplitude of $A_2 \approx A_1$, and a swing frequency at $f_2 \approx f_1$, or it does not swing together with the fish body with an amplitude of $A_3 < 0.17L$, and a swing frequency at $f_3 = 3.0 \sim 7.0 f_1$. The left and right pectoral fins move back and forth or flap up and down, and the flap frequencies are $f_4 = 0.5 \sim 1.0 f_1$ and $f_5 = 0.5 \sim 1.0 f_3$.

(2) To retreat, the koi mainly depends on the back and forth and up and down strokes of the left and right pectoral fins, while the fish body and tail fin provide low contribution. The left pectoral fin's back and forth stroke frequency is 2 Hz< f_6 <3 Hz, yet the right pectoral fin is not highly synchronized with the left pectoral fin, and its back and forth stroke frequency is 2 Hz< f_7 <3 Hz, where $f_6 \neq f_7$. The asynchrony of the left and right pectoral fins is one of the main reasons for the koi's tortuous retreating path.

(3) When the koi turns left (right), it is mainly done by rapid fish body and tail fin movements. The fish body significantly bends, with a bending amplitude upper limit as $0.6L$. Together with the body, the caudal fin significantly bends with the bending amplitude upper limit as $0.4L$. At the same time, the right (left) pectoral fin is retracted to the fish belly, while the left (right) pectoral fin is kept away from the fish belly.

(4) When the koi floats up, the fish body swings left and right with the amplitude $A_4 < 0.27L$ and the swing frequency f_8 <0.5 Hz. At the same time, the caudal fin swings left and right with the amplitude $A_5 < 0.17L$ and the swing frequency f_9 <0.5 Hz, where $f_8 \approx f_9$. The left and right pectoral fins flap up and down, while the flap frequency of the left pectoral fin is f_{10} <2 Hz and the flap frequency of the right pectoral fin is f_{11} <2 Hz, where $f_{10} \neq f_{11}$.

During all these processes, each fin undergoes complex deformation, and the deformation includes complex fin surface fluctuations. These complex deformations are mainly to maintain the balance of the fish body and control the moving directions.

Discussion

In this section, combining with fish body wave model, the fish body wave characteristics of the three koi swimming states are analyzed. The measured fish body waves are quite different from the theory. There are two main reasons: first, in actual observation, even if the researchers set many conditions to restrict the movement of the fish, the fish will not follow the planned route. The measured fish wave curve is still consistent with the actual swimming rule of koi, and the changes of the fish wave can be observed from the curves; second, the model is too simple to describe the fish wave characteristics completely. From the fish body wave model established based on the viscoelastic beam theory described before, it can be seen that the complexity of a simplified fish body wave model is already very high. Therefore, there are still lots of research works to be carried out for studying fish body wave model.

This section also studies fish movement in combining with the proposed discrete model. The discrete model of fish body-fin synergistic propulsion mainly focuses on the qualitative description of the fish body-fin synergistic propulsion mechanism, which has a particular reference value for the research on the control method of underwater robots. Nevertheless, the model still has many limitations, such as the model cannot reveal the mechanism of fish movement from the inside of fish. For the study of fish movement, from an experimental point of view, some more essential features may be found through the fusion of various types of sensor data. Although multi-source sensor data fusion is complex, the existing multi-modal learning technology provides an important idea for solving this problem. For example, combining information from two modalities of infrared thermal imaging and pose estimation may help to quantify fish movement.

CONCLUSION

In this study, a fish pose and motion parameter estimation platform is first constructed to quantify the motion of fish and to provide solid data support for analyzing the propulsion mechanism of fish body and fins. The platform mainly includes raw data collection of fish movement and fish movement quantification algorithms. Secondly, this study establishes a discrete model to qualitatively describe fish body-fin propulsion, which provides a solid theoretical basis for analyzing the synergistic propulsion mechanism of fish body and fins. Finally, this study takes the koi body-fin synergistic propulsion mechanism as an example in the still water environment and mainly analyzes the fish body wave characteristics of the three koi swimming states (advancing, retreating, and turning). In addition, the state matrices of the koi, showing the relationships between swimming states (advancing, retreating, turning, and floating up) and the motion parameters corresponding to each fin, are determined. The experiments obtain a simple body-fin coordination mechanism corresponding to the four koi swimming states.

The platform constructed in this study provides new ideas for fish movement research, and the research results have particular significance for designing, developing, and optimizing new underwater robots.

In addition, there are still some follow-up questions. This paper only studies the fish movement in still water environment. The experiments can be extended to flowing water and other more complex environments. In addition, some more essential results may be achieved through the fusion of various types of sensor data, and related technologies based on multi-source information fusion may be able to promote neurobiological research vigorously. Existing multimodal learning techniques may provide some valuable experiences for processing multi-source data. For example, combining information from three modalities of particle image, infrared thermal imaging, and pose estimation may help to quantify fish movement and discover the nature of fish swimming from the inside out.

Competing interests

The authors declare no competing or financial interests.

Funding

The *Major Science and Technology Projects in Sanya*(ZDKJ-SY-2020-001), the *Scientific Research Foundation of Hainan Tropical Ocean University*(No. RHDRC202001) and the *Major Science and Technology Projects of Hainan Province*(ZDKJ202017-02-01) have funded my research.

Data availability

Please refer the project to https://github.com/wux024/AdamPose and https://github.com/wux024/AdamPosePlug.

REFERENCES

Bandyopadhyay, P. R. (2005). Trends in biorobotic autonomous undersea vehicles. *IEEE Journal of Oceanic Engineering*, 30(1):109–139.

Bogue, R. (2015). Underwater robots: a review of technologies and applications. *Industrial Robot: An International Journal*, 42:186–191.

Cheng, X. E., Du, S. S., Li, H. Y., Hu, J. F., and Chen, M. L. (2018). Obtaining three-dimensional trajectory of multiple fish in water tank via video tracking. *Multimedia Tools and Applications*, 77:24499–24519.

Liu, X., Yue, Y., Shi, M., and Qian, Z.-M. (2019). 3-D video tracking of multiple fish in a water tank. *IEEE Access*, 7:145049–145059.

Mao, J., Xiao, G., Sheng, W., Qu, Z., and Liu, Y. (2016). Research on realizing the 3D occlusion tracking location method of fish's school target. *Neurocomputing*, 214:61–79.

Nguyen, P. L., Lee, B. R. (2013). Dynamic modeling of a non-uniform flexible tail for a robotic fish. *Journal of Bionic Engineering*, 10(2):201–209.

Qian, Z.-M. and Chen, Y. Q. (2017). Feature point based 3d tracking of multiple fish from multi-view images. *PLOS ONE*, 12(6):1–18.

Saberioon, M. and Cisar, P. (2016). Automated multiple fish tracking in three-dimension using a structured light sensor. *Computers and Electronics in Agriculture*, 121:215–221.

Valdivia y Alvarado, P. P. A. (2007). *Design of biomimetic compliant devices for locomotion in liquid environments*. PhD thesis, Massachusetts Institute of Technology, Massachusetts.

Voesenek, C. J., Pieters, R. P. M., and van Leeuwen, J. L. (2016). Automated reconstruction of three-dimensional fish motion, forces, and torques. *PLOS ONE*, 11(1):1–17.

Wang, L., Xu, M., Liu, B., Low, K. H., Yang, J., and Zhang, S. (2013). A three-dimensional kinematics analysis of a koi carp pectoral fin by digital image processing. *Journal of Bionic Engineering*, 10(2):210–221.

Weaver Jr, W., Timoshenko, S. P., and Young, D. H. (1991). *Vibration problems in engineering*. John Wiley & Sons, New Jersey.

Westneat, M. W., Hoese, W., Pell, C. A., and Wainwright, S. A. (1993). The horizontal septum: mechanisms of force transfer in locomotion of scombrid fishes (scombridae, perciformes). *Journal of Morphology*, 217(2):183–204.

Wu, G. (2010). Measuring the three-dimensional kinematics of a free-swimming koi carp by video tracking method. *Journal of Bionic Engineering*, 7(1):49–55.

Wu, X., Wang, Y., Chen, L., Zhang, L., and Wang, L. (2022). Motion parameters measurement of user-defined key points using 3D pose estimation. *Engineering Applications of Artificial Intelligence*, 110:104667.

Yu, J., Wang, M., Dong, H., Zhang, Y., and Wu, Z. (2018). Motion control and motion coordination of bionic robotic fish: A review. *Journal of Bionic Engineering*, 15:579–598.